



# Sulfur cycling in freshwater sediments: A cryptic driving force of iron deposition and phosphorus mobilization

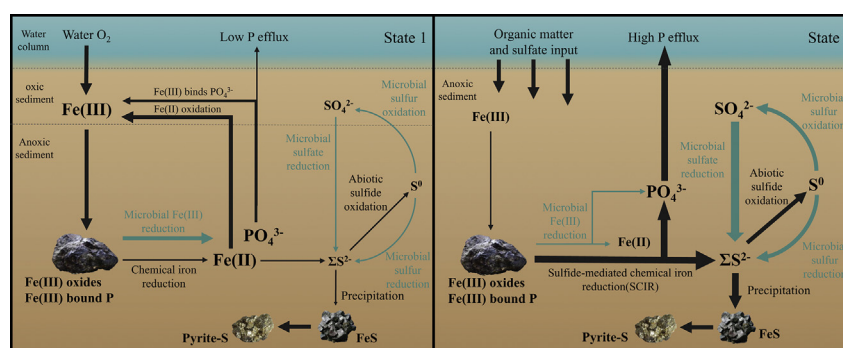
Songjun Wu<sup>1</sup>, Yanping Zhao<sup>1</sup>, Yuanyuan Chen, Xiumei Dong, Mingyue Wang, Guoxiang Wang\*

Jiangsu Center for Collaborative Innovation in Geographical Information Resource Development and Application, Jiangsu Key Laboratory of Environmental Change and Ecological Construction, School of Environment, Nanjing Normal University, Nanjing 210023, China

## HIGHLIGHTS

- Acetate addition significantly stimulated SRB growth and varied the sulfur cycling.
- Microbial iron reduction was blocked with evidence of depressed IRB, Fe(II) release.
- Sulfide-mediated chemical iron reduction dominated the iron reduction in the system.
- Phosphorus mobilization was promoted because of the sulfur-mediated iron reduction.
- $\Sigma S^{2-}$  precipitation before diffusion led to the  $\Sigma S^{2-}$ -missing sulfur cycling.

## GRAPHICAL ABSTRACT



## ARTICLE INFO

### Article history:

Received 9 October 2018

Received in revised form 10 December 2018

Accepted 10 December 2018

Available online 11 December 2018

Editor: Jay Gan

### Keywords:

Sulfur cycling  
Sulfate-reducing bacteria  
Iron reduction  
Phosphorus mobility  
Freshwater ecosystem

## ABSTRACT

Sulfur cycling in freshwater ecosystems has been previously considered minor, and the direct evidence of its impacts on iron and phosphorus cycles in freshwater sediments remains unclear. In this study, mesocosms with amended acetate and various sulfate concentrations ( $1.5\text{--}3.0\text{ mmol L}^{-1}$ ) were set up to investigate sulfur cycling and its influences on iron-rich freshwater sediments. Acetate addition induced hypoxia and provided substrates, which stimulated the sulfur cycling with evidence of  $\text{SO}_4^{2-}$  decline,  $\Sigma S^{2-}$ ,  $\text{S}^0$  increase and corresponding variations of sulfate-reducing bacteria (SRB) and sulfur-oxidizing bacteria. Meanwhile, the growth of iron-reducing bacteria (IRB) was suppressed, and lower Fe(II) release was correspondingly related to larger SRB abundance at higher sulfate level, indicating that microbial iron reduction might be blocked by SRB activities. However, continuous dissolution of Fe(III) oxides and generation of iron sulfides were observed, suggesting that sulfide-mediated chemical iron reduction (SCIR) became the dominant iron-reducing pathway, and Fe(II) was buried as iron sulfides instead of released to water column, which resulted in a transition of iron cycling into unidirectional SCIR. Consequently, continuous dissolution of Fe(III) oxides led to significant increase of  $\text{PO}_4^{3-}$  concentration in the water column and sediment pore-water, revealing the phosphorus mobility in sediments derived from the SCIR process. To note, sustained accumulation of iron sulfides was observed even without  $\Sigma S^{2-}$  presence, suggesting that  $\Sigma S^{2-}$  precipitation occurred prior to diffusion. Thus,  $\Sigma S^{2-}$ -missing sulfur cycling seemed “cryptic” in this study. To highlight, the transition of the iron-reducing pathway and resulting  $\text{PO}_4^{3-}$  release can be induced even under current sulfate level of Lake Taihu, and elevated sulfate levels could significantly intensify SCIR and phosphorus mineralization. Thus, the stimulated iron deposition and the resulting phosphorus release derived from the sulfur cycling should be paid more attention to in the treatment of eutrophic freshwater ecosystems.

© 2018 Published by Elsevier B.V.

\* Corresponding author at: 1, Wenyuan Road, Xianlin University District, Nanjing 210023, China.

E-mail address: [wangguoxiang@njnu.edu.cn](mailto:wangguoxiang@njnu.edu.cn) (G. Wang).

<sup>1</sup> These authors contributed to this manuscript equally and should be regarded as co-first authors.

## 1. Introduction

Phosphorus, which is needed for DNA, RNA and energy transfer, was essential in aquatic ecosystems (Conley et al., 2009) and its excess has aroused broad concern, which is primarily responsible for frequent eutrophication (Correll and David, 1998). Various factors were demonstrated to influence the phosphorus cycling, including ubiquitous iron and sulfur (Baldwin and Mitchell, 2012; Flores-Alsina et al., 2016).

Positive proportions between dissolved ferrous ions (Fe(II)) and phosphate ( $\text{PO}_4^{3-}$ ) have been widely reported in both freshwater and marine ecosystems (Mort et al., 2010; Vali, 2006). The strong correlation is proved between iron and phosphorus cycling as iron hydroxides have a high capacity of absorption which results in phosphorous deposition while iron reduction stimulates the dissolution of sedimentary iron and release of adsorbed phosphorus (Mort et al., 2010). The latter process, which involves the reduction of dissolved ferric ions (Fe(III)) and consumption of iron minerals is mostly dominated by iron-reducing bacteria (IRB) (Bo, 2000). Thus, iron cycling, including microbial iron reduction and physicochemical precipitation of Fe(III), controlled phosphorus cycling in the preindustrial non-sulfidic sediments to a certain extent (Olsson et al., 1997).

However, sulfur was involved in iron-phosphorus cycling after the explosive increases of sulfur input due to developing industry (Hall et al., 2006). Sulfur cycling was consequently stimulated and considering that microbial iron and sulfate reduction both favor anaerobic environment, competition is likely to occur between IRB and SRB with limited substrates. Inhibition of IRB populations by SRB has been previously reported, and consequently, microbial iron cycling was blocked and substituted by sulfide-mediated chemical iron reduction (SCIR) (Hansel et al., 2015; Koretsky et al., 2003; Man et al., 2014). The crucial difference between microbial iron reduction and SCIR is the destination of reduced ferric ions (Fe(III)), which ultimately dissolve into the water via former pathway or precipitate with sulfides via latter pathway (Lehtoranta et al., 2009). Thus, without released Fe(II) and newly-generated Fe(III) in the water column, iron cycling would be blocked and turned to unidirectional SCIR. A vicious circle would form as the intensive dissolution of iron-binding phosphorus due to SCIR could cause aggravation of water eutrophication (Chen et al., 2016), while resulting larger algal blooms provide sustained hypoxia and substrates that fuel SRB as the primary driving force of SCIR (Anderson et al., 2009). Moreover, as pyrite-S are permanently buried under anoxic conditions, diminishing the capacity of  $\text{PO}_4^{3-}$  absorption due to lack of Fe(III) regeneration will lead to an irreversible deterioration (Canfield, 1989; Gunnars et al., 2002). Extreme cases are the spreading dead zones in marine environments with severe eutrophication and lasting hypoxia, which were reported from >400 systems and affecting a total area of >24,500 km<sup>2</sup> (Diaz and Rosenberg, 2008; Schobben et al., 2016).

Such transition due to SCIR was mostly studied in marine ecosystem (Glombitza et al., 2016; Hyacinthe and Cappellen, 2004; Thamdrup et al., 1994). However, sulfur cycling in freshwater ecosystems was considered minor, and researches on its impacts remained incomplete, which were attributed to the depressed sulfate reduction enslaved to low sulfate levels and theoretically predicted prior utilization of substrate by IRB according to Gibbs energy ( $\Delta G_r$ ) calculations (Nakagawa et al., 2012). The central tenant in microbial biogeochemistry suggests that microbial metabolisms follow a predictable sequence of terminal electron acceptors based on the energetic yield (Hansel et al., 2015). Under the umbrella of classic redox tower, microbial respiration of Fe(III) is expected to outcompete sulfate in all but high-sulfate systems. Thus, the influence of sulfur cycling has been considered negligible in the freshwater ecosystem (Hoehler et al., 1998; Lovley and Phillips, 1988; Patrick and Henderson, 1981). However, recent studies found the sustained respiration of sulfur species accompanied by the iron reduction (Straub and Schink, 2004; Lohmayer et al., 2014). It has demonstrated that sulfate reduction could be preponderant in sediments under low sulfate concentrations, regardless of iron oxides present

(Hansel et al., 2015). And an in-situ environmental deterioration due to SCIR has been discovered in a freshwater lake with increasing sulfate concentration in the Netherlands (Moosmann et al., 2006). Thus, considering the sulfate ( $\text{SO}_4^{2-}$ ) concentrations reported to increase throughout the world via atmospheric deposition and agricultural discharge (Paerl and Paul, 2012), sulfur cycling probably plays a vital role in freshwater ecosystems.

Some recent studies have focused on the effects of biogeochemical cycling of iron and sulfur on the phosphorus mobility in freshwater sediments during the algae decomposition by carrying out a mesocosm experiment with the addition of algae (Chen et al., 2016; Chen et al., 2018; Han et al., 2015). However, numerous materials would be liberated by algae decomposition. As the materials derived from decomposed algae and sediments are hard to be distinguished, the algae addition enhances the difficulty in investigating relative anaerobic respiration in sediments, so it is difficult to provide the direct evidence to indicate the phosphorus mobility resulted from the varying S and Fe cycling. Thus, a mimicking mesocosm experiment without exogenous S, Fe and P is necessary to clearly investigate the interactions of S and Fe and the related phosphorus mobility in sediment.

In this study, mesocosms were set up with lake water and sediments collected from Lake Taihu. The incubation lasted for 19 d with added acetate instead of algae. Both iron and sulfur cycles in sediments were investigated at four sulfate levels (1.5–3.0 mmol L<sup>-1</sup>). Moreover, SCIR and subsequent crucial effects on  $\text{PO}_4^{3-}$  release were also studied. This study will help to evaluate sulfur cycling and its impacts on iron and phosphorus with organic matter addition at various sulfate levels.

## 2. Materials and methods

### 2.1. Sample collection

Samples were collected from the eutrophic Lake Taihu, one of the largest shallow freshwater lakes in China with an area of 2340 km<sup>2</sup> and a mean depth of 1.9 m (Qin et al., 2007). Both water and sediments were gathered near the Port Maodu in the western lake (31°24'32"N, 120°1'55"E) with a line distance of 1 km to the shore. Sediment cores were collected using a gravity core sampler and immediately sectioned into 3 cm intervals. Lake water was collected at 30 cm below the water surface into polyethylene bottles using a pump. Both water and sediment samples were kept in a portable refrigerator and delivered to the laboratory within 2 h and stored at 4 °C for no longer than 24 h before measurement.

### 2.2. Mesocosms experiment

The mesocosms set-ups consisted of four perspex cylindrical containers (9 cm diameter, 60 cm high). Each container was processed in advance with boreholes on one side, which allowed seven pore water samplers (Rhizon, Netherlands) inserted in to collect pore water samples at depths of 0.5, 1.5, 2.5, 3.5, 6.5, 10 cm below the water-sediment interface (WSI). A glass tube was placed in to collect the water sample (5 cm above WSI). All samplers were fixed to prevent the disturbance to sediments. Stratified sediment was sieved through a strainer of 100 mesh, subsequently homogenized and put separately into each container to reach a thickness of 20 cm. Lake water was gently added to a thickness of 30 cm using intravenous needles. A 7-day-preincubation at 25 °C was taken. During this period, concentrations of  $\Sigma\text{S}^{2-}$ ,  $\text{SO}_4^{2-}$ ,  $\text{PO}_4^{3-}$ , Fe(II) in overlying and pore water were measured every day to test the stability of the system.

After preincubation, 10 mM carbon of acetate was added to the water columns as the electron donor.  $\text{Na}_2\text{SO}_4$  was subsequently dissolved in the water columns as follows: no addition (1.5S), 0.5 mmol  $\text{SO}_4^{2-}$  L<sup>-1</sup> (2.0S), 1.0 mmol  $\text{SO}_4^{2-}$  L<sup>-1</sup> (2.5S), and 1.5 mmol  $\text{SO}_4^{2-}$  L<sup>-1</sup> (3.0S). All columns were incubated at 30 °C in the dark for 19 days. During this period, measurements of DO and ORP in

overlying water and sediment pore water were performed using needle-type microelectrodes (Unisense, Denmark). Thereafter, overlying water was sampled twice (9:00 and 21:00) per day, while pore water was sampled every two days to investigate inorganic elements ( $\text{SO}_4^{2-}$ ,  $\Sigma\text{S}^{2-}$ ,  $\text{PO}_4^{3-}$ , Fe(II)). A microscale-method was realized using microplate reader (Biotek, America) to minimize the sampling volume. 3 mL of overlying and pore water were sampled each time respectively, and pure water of the same volume was added.

Sediment samples were sectioned in glove boxes on days 1, 2, 4, 6, 8, 10, 12, 18 for subsequent analysis on sedimentary phosphorous (TP, Fe-P), sulfur (AVS, Pyrite-S and  $\text{S}^0$ ) and iron oxides (ferrihydrite-Fe, total Fe (III) oxides). DNA extraction was carried out after sediment sampling.

### 2.3. Chemical analytical methods

All samples of the water column and pore water were filtered through 0.45  $\mu\text{m}$  filters before measurement.  $\text{SO}_4^{2-}$  was detected using a turbidimetric method (Tabatabai, 1974).  $\Sigma\text{S}^{2-}$  was analyzed using the methylene blue method (Cline, 1969).  $\text{PO}_4^{3-}$  was determined using the molybdenum blue method (Chen et al., 2016) and Fe(II) was analyzed colorimetrically (Lovley and Phillips, 1988). Dissolved organic carbon (DOC) and dissolved inorganic carbon (DIC) were investigated using a TOC analyzer (Analytik Jena HT1300).

Sedimentary contents of S, Fe and P were also investigated. Briefly, TP content in sediments was investigated as  $\text{PO}_4^{3-}$  after acid hydrolysis at 340 °C (Murphy et al., 1962). Sedimentary iron oxides including Ferrihydrite-Fe and total Fe(III) oxides were analyzed as the material leached from ascorbic acid solution and dithionite solution, respectively (Rozan et al., 2002) and reduced inorganic sulfur were determined using a sequential extraction method (Hsieh and Shieh, 1997).

### 2.4. DNA extraction for Illumina sequencing and real-time quantitative PCR (RT-QPCR)

Surface sediments (0–1 cm) from four columns were collected on day 0, 6, 12, 18 to investigate the microbial community and abundance of SRB. DNA from sediment samples were extracted with the PowerSoil DNA isolation kit (MO BIO Laboratories, Inc.) following the manufacturer's manual. All extracted DNA was quantified with Nanodrop 2000 (Thermo Scientific) and stored at –20 °C for further analysis.

In order to investigate the variation of microbial communities, the technique of Illumina sequencing was used. Briefly, the V3-V4 hyper-variable regions of the bacterial 16S rRNA gene were amplified with primers 515F and 907R. The PCR incubation conditions were as follows: 95 °C for 2 min, followed by 25 cycles of 95 °C for 30 s, 55 °C for 30 s and 72 °C for 30 s with a final extension of 72 °C for 5 min, 10 °C until halted by the user. OTUs were assigned using a clustering protocol of UCLUST with 97% similarity threshold. All sequences were deposited in the NCBI Sequence Read Archive (SRA) database (Accession number: SRA158647).

The *dsrB*-targeted RT-PCR technique, performed in Step-one Plus Real-Time PCR Machine (Applied Biosystems), was used to determine the abundance of SRB in sediments. The primer pair for *dsrB* was DSRp2060F/DSR4R. The reactions were performed at 95 °C for 5 min followed by 20 cycles of 95 °C for 40 s, 60 °C decrease to 50 °C with 0.5 °C unit for each cycle, 72 °C for 1 min, and 20 cycles of 95 °C for 40 s, 50 °C for 40 s, 72 °C for 1 min, 4 °C forever at the end.

### 2.5. Statistical analyses

Statistically significant differences were determined by one-way-analysis of variance using Origin Pro 7.5 and SPSS 19.0 software. A  $P < 0.05$  was considered significant. Illumina sequencing data analysis was done using QIIME 1.8.0 software.

## 3. Results

### 3.1. Dynamics of dissolved carbon and physical parameters (DO, ORP)

The concentrations of DTC and DOC in lake water were 20.47, 11.73  $\text{mg L}^{-1}$ , respectively. High levels of DOC (135.83  $\text{mg L}^{-1}$  in average on day 0) were attributed to acetate addition. Decreases of DTC and DOC were observed in the water column during whole incubation. On day 19, the average concentrations of DTC and DOC were 81.07  $\text{mg L}^{-1}$  and 19.83  $\text{mg L}^{-1}$  (Fig. 1), which were 48.13% and 85.40% lower than the initial concentration. In contrast, DIC gradually increased to 61.24  $\text{mg L}^{-1}$  during 19-d incubation (Fig. 1), suggesting a microbial-transition from DOC to DIC. We did not find significant impacts of amended sulfate on variations of dissolved carbon in the water column.

Microelectrode-measured DO and ORP profiles were investigated to evaluate the redox conditions in sediments. DO in overlying water and sediments declined to below 4.0  $\mu\text{mol L}^{-1}$  after the addition of acetate for 6 days (Fig. 2), suggesting a fast-formed anoxic condition in sediment caused by the decomposition of organic matter. The hypoxia in sediments sustained until the end of incubation while the re-oxygenation in the water column was found on day 19. There was no significant change in DO at different sulfate levels.

ORP variations in sediments revealed strong relations with depth. There was a regular pattern for all incubated groups that ORP decreased gradually with increasing depth from 0 to 5 cm below the WSI at the initial stage (Fig. 2b). However, the depth dependency was reversed after acetate and sulfate addition. Consistent decreases were observed during the first 6 days, reflecting a fast-formed reductive condition in sediments. Thereafter, the ORP in overlying water and sediments exhibited uptrends over the next 12 days. In contrast with unaffected DO, elevated sulfate levels had impacts on ORP variation. Sharp recoveries of ORP in the sediment of 0–1 cm occurred on days 8 (1.5S), 10 (2.0S), 10 (2.5S), 12 (3.0S), respectively. It was clear that additional sulfate facilitated ORP decline and resisted the subsequent recovery.

### 3.2. Concentrations of soluble Fe, S and P in the water column

Variations of  $\text{SO}_4^{2-}$ ,  $\Sigma\text{S}^{2-}$ , Fe(II) and  $\text{PO}_4^{3-}$  in the water column during the experimental period are presented in Fig. 3. Acetate addition significantly influenced variations of  $\text{SO}_4^{2-}$  and  $\Sigma\text{S}^{2-}$  concentrations in overlying water.  $\text{SO}_4^{2-}$  in overlying water dramatically declined on the first 4 days after acetate addition and gradually stabilized at  $885.93 \pm 19.78$  (1.5S),  $1027.97 \pm 25.46$  (2.0S),  $1367.38 \pm 34.20$  (2.5S),  $1390.07 \pm 32.81$  (3.0S)  $\mu\text{mol L}^{-1}$  at the end of the experiment. An inverse pattern of  $\Sigma\text{S}^{2-}$  was observed with a rapid increase prior to intensive

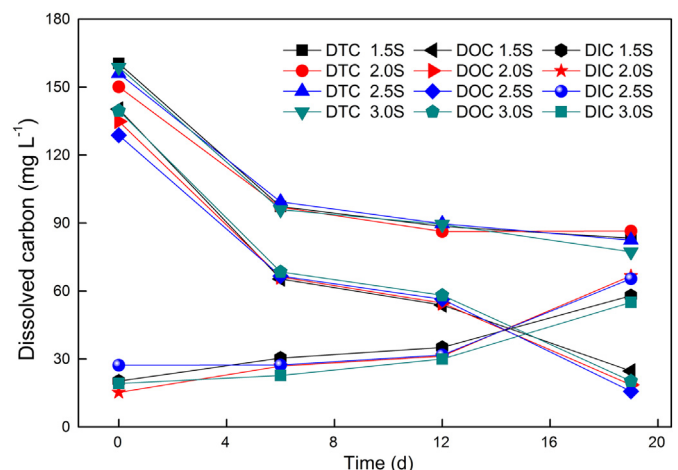


Fig. 1. DTC, DOC and DIC concentrations in the water column during incubation.

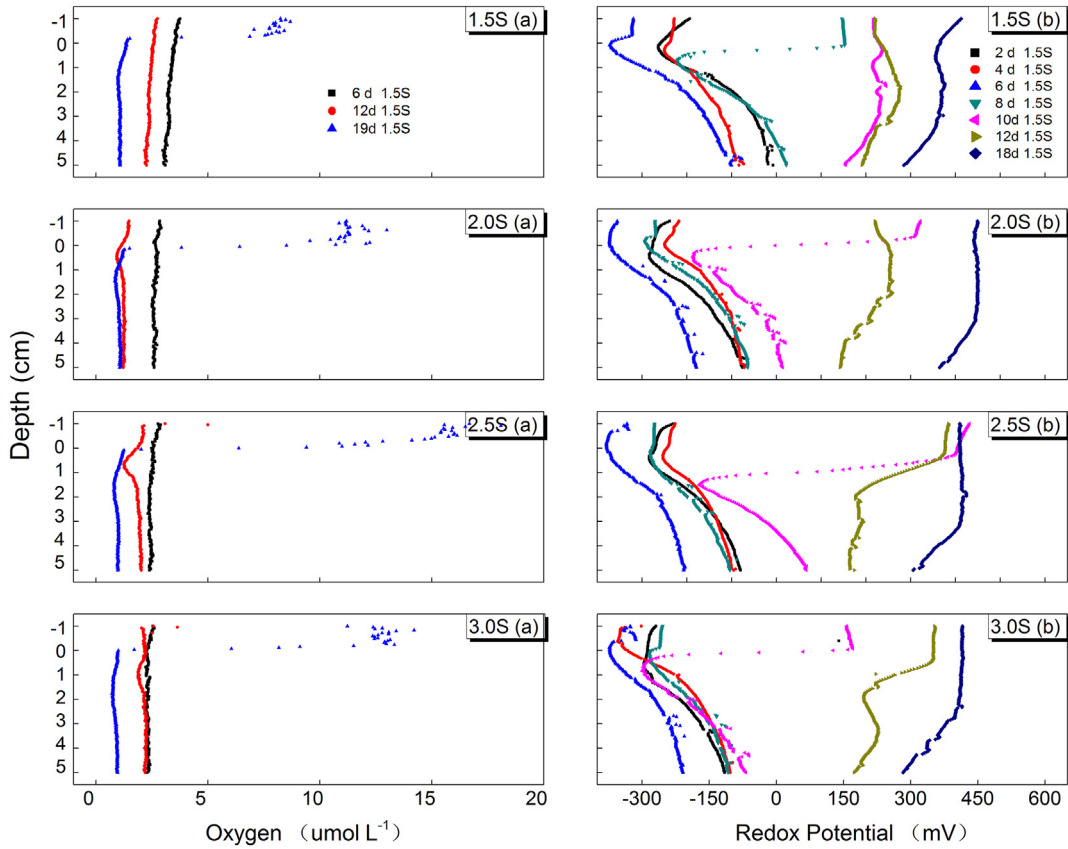


Fig. 2. Variations of DO (a) and ORP (b) in overlying water (−1–0 cm) and sediments (0–5 cm) during incubation.

decline. Slight increases were observed on the first 4 days followed by sharp increases up to day 11 with maximum values of  $129.84 \pm 4.71$  (1.5S),  $137.27 \pm 6.32$  (2.0S),  $266.32 \pm 1.35$  (2.5S) and  $351.02 \pm 12.05$

(3.0S)  $\mu\text{mol L}^{-1}$ , respectively. After that, the  $\Sigma\text{S}^{2-}$  dramatically decreased to  $<10 \mu\text{mol L}^{-1}$  after day 15. As expected, higher  $\Sigma\text{S}^{2-}$  concentration was observed at higher  $\text{SO}_4^{2-}$  concentration throughout the

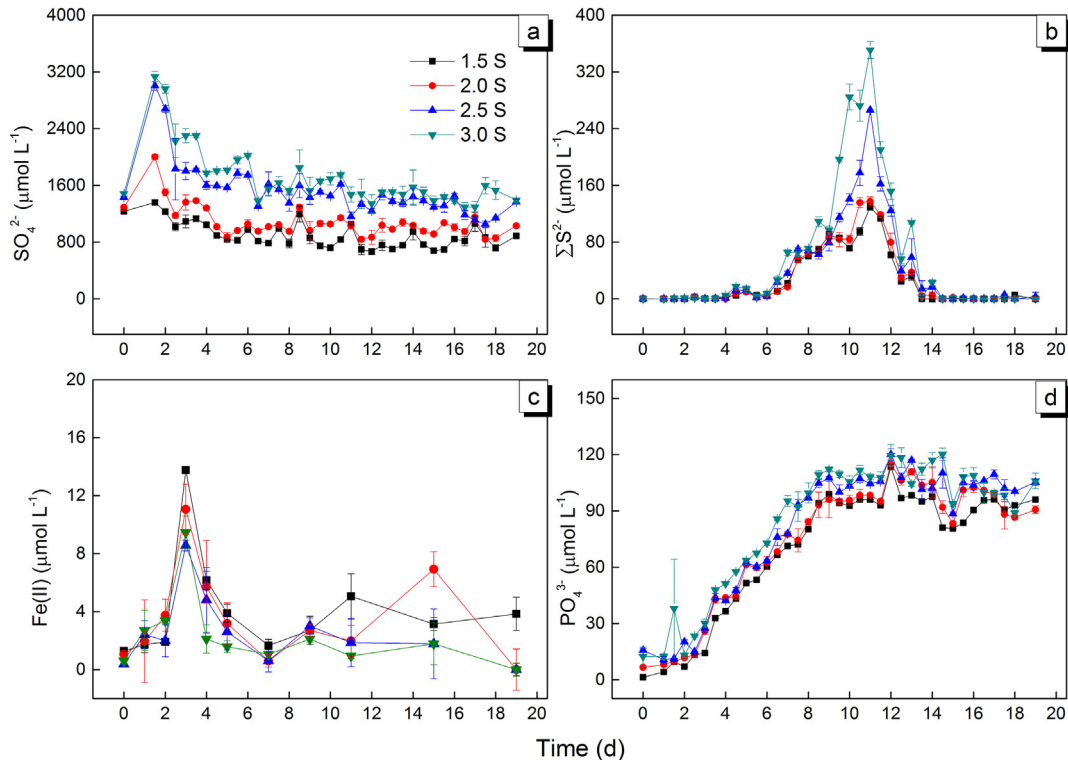


Fig. 3. Variations of  $\text{SO}_4^{2-}$  (a),  $\Sigma\text{S}^{2-}$  (b), Fe(II) (c) and  $\text{PO}_4^{3-}$  (d) in the water column during incubation.

incubation. To note is that although  $\text{SO}_4^{2-}$  variations revealed inverse trends to  $\Sigma\text{S}^{2-}$ , the decreased concentrations of  $\text{SO}_4^{2-}$  were 3–7 times of generated  $\Sigma\text{S}^{2-}$ , revealing the occurrence of sulfide metabolic pathways like precipitation or gasification.

Variation of Fe(II) concentrations in water column exhibited arched shapes with uptrend on days 0 to 3 and downtrend on days 3 to 7 (Fig. 3c). At the end of the experiment, Fe(II) concentrations in the water column remained at a relatively low level ( $2.08 \pm 0.86 \mu\text{mol L}^{-1}$  in average). In addition, Fe(II) peak values reached  $13.75 \pm 1.13$  (1.5S),  $11.04 \pm 0.37$  (2.0S),  $8.57 \pm 1.74$  (2.5S) and  $9.47 \pm 0.00$  (3.0S)  $\mu\text{mol L}^{-1}$  on day 3 and lower Fe(II) concentrations were observed at higher sulfate concentrations since day 3, suggesting that elevated sulfate levels promoted the limitation of Fe(II) release.

Organic matter addition significantly stimulated  $\text{PO}_4^{3-}$  dissolution to overlying water.  $\text{PO}_4^{3-}$  concentrations gradually increased from the initial value of  $6.64 \pm 0.58 \mu\text{mol L}^{-1}$  to 472.64 (1.5S), 507.79 (2.0S), 530.45 (2.5S) and 574.57 (3.0S)  $\mu\text{mol L}^{-1}$  on day 11. It is clear that higher  $\text{PO}_4^{3-}$  release was related to higher amended sulfate. Slight decreases were observed since day 14, with final concentrations of  $99.49 \pm 2.08 \mu\text{mol L}^{-1}$  on average.

### 3.3. Concentrations of soluble S, Fe and P in sediment pore-water

The depth profiles of  $\text{SO}_4^{2-}$ ,  $\Sigma\text{S}^{2-}$ , Fe(II) and  $\text{PO}_4^{3-}$  in sediment pore-water were investigated. Initial profiles of  $\text{SO}_4^{2-}$  at the vicinity of WSI showed a strong downtrend with depth, which was related to the reductive condition in deeper sediments (Fig. 4).  $\text{SO}_4^{2-}$  concentrations in all treatments rapidly decreased to  $<156.51 \pm 6.03 \mu\text{mol L}^{-1}$  on day 3. Lower  $\text{SO}_4^{2-}$  concentrations were observed during the rest of incubation in all treatments.

In contrary to the vertical distribution of  $\text{SO}_4^{2-}$ ,  $\Sigma\text{S}^{2-}$  gradually increased with depth. Similar to the  $\Sigma\text{S}^{2-}$  variation in the water column,  $\Sigma\text{S}^{2-}$  concentration in sediment pore-water also increased after acetate addition and reached maximum on day 11 (Fig. 4b). The peak values of  $\Sigma\text{S}^{2-}$  were  $50.71 \pm 4.71$  (1.5S),  $53.90 \pm 6.32$  (2.0S),  $57.62 \pm 1.35$  (2.5S),  $72.75 \pm 12.05$  (3.0S)  $\mu\text{mol L}^{-1}$ , respectively. It is clear that sulfate addition promoted the  $\Sigma\text{S}^{2-}$  generation.

The vertical distributions of Fe(II) in sediment pore-water showed downward increases in concentration with depth (Fig. 4c), indicating the reductive dissolution of iron oxides under anoxic conditions. Unlike the fluctuant dynamics in the water column, Fe(II) concentrations in sediment pore-water revealed sustained downtrends during incubation. Fe(II) decreased by 50.53% (1.5S), 54.65% (2.0S), 73.54% (2.5S), 62.68% (3.0S) after 19-d incubation. Besides, lower Fe(II) concentrations in sediments were observed at higher amended sulfate, especially in upper sediments (0–1 cm), indicating a significant suppression on Fe(II) release by elevated sulfate.

$\text{PO}_4^{3-}$  in sediment pore-water mainly concentrated in the surface sediment of 0–1 cm, with concentrations higher than those in upward overlying water or downward sediment pore-water (Fig. 4d). After acetate addition,  $\text{PO}_4^{3-}$  concentration at the vicinity of WSI gradually increased to the maximum on day 11 and decreased since then. The peak values of  $\text{PO}_4^{3-}$  in 0–1 cm sediment pore-water on day 11 were  $591.33 \pm 6.45$  (1.5S),  $692.89 \pm 10.62$  (2.0S),  $748.59 \pm 5.79$  (2.5S) and  $767.42 \pm 9.05$  (3.0S), respectively. It is clear that higher  $\text{PO}_4^{3-}$  concentration was related to higher amended sulfate, suggesting  $\text{SO}_4^{2-}$  addition promoted the phosphorus dissolution. Approximately 26.27% increase of  $\text{PO}_4^{3-}$  was attributed to per mole of elevated  $\text{SO}_4^{2-}$  on average.

### 3.4. Contents of S, Fe and P in sediment

AVS, Pyrite-S and  $\text{S}^0$  were measured to investigate sulfur cycling in sediments. In general, distributions of sedimentary sulfur in sediments were consistent, reflecting in the highest content in surface sediments and decreasing content with increasing depth (Fig. 5). This result

indicated that sulfides formation and precipitation mainly occurred in surface sediments. Moreover, the three types of solid sulfur gradually increased with incubation time. The most active accumulation was observed in surface sediments during incubation, and higher content was observed at higher amended sulfate. The concentrations of AVS, Pyrite-S and  $\text{S}^0$  on surface sediments were up to  $170.12 \mu\text{mol g}^{-1}$ ,  $34.35 \mu\text{mol g}^{-1}$  and  $7.85 \mu\text{mol g}^{-1}$  on day 18, respectively (Fig. 5).

Contents of TP, Fe-P, ferrihydrite-Fe and total Fe(III) oxides in 0–2 cm sediments were monitored on day 0 and day 19 to investigate iron and phosphorus pool in sediments (Table 1). Generally, their contents in surface sediments decreased after the 19-day incubation, and the greater decreased content was observed at higher amended sulfate. Compared with the initial value, Fe-P contents were reduced by 7.9% (1.5S), 17.1% (2.0S), 33.3% (2.5S) and 35.0% (3.0S), respectively. The percentages of Fe-P in TP were also respectively dropped from the initial 25.0% to 23.4% (1.5S), 23.6% (2.0S), 20.1% (2.5S) and 20.4% (3.0S), indicating that elevated sulfate levels enhanced the desorption of iron bound phosphorus, mostly Fe-P. Similar dissolution of sedimentary iron was observed. Total Fe(III) oxides decreased by 4.50% (1.5S), 7.49% (2.0S), 5.18% (2.5S) and 12.22% (3.0S) while ferrihydrite-Fe decreased by 12.20% (1.5S), 9.57% (2.0S), 22.24% (2.5S) and 25.59% (3.0S), respectively. Evidently, elevated sulfate levels promoted dissolution of iron oxides.

### 3.5. Microbial communities and quantification of SRB in sediments

In order to confirm the relative bacterial respiration with elevated sulfate levels, sequencing and RT-QPCR technologies were used to determine the microbial communities on days 0, 6, 19 and the cell copy numbers of SRB on days 0, 6, 12, 19 in surface sediments (0–1 cm).

Sequencing data showed significant differences in microbial communities before/after incubation (Fig. 6). In the initial sediments, iron reducer *Geobacter* was the most abundant genera among relative respiration groups (sulfate-reducing, iron-reducing, and methanogenesis). The average abundance of *Geobacter* was 1.29%, which was 111.99%, 77.26% higher than the most abundant SRB (*Desulfobulbus*) and SOB (*Sulfurisoma*) genera. Classified methanogen genera were <0.3%. Strong changes were observed after acetate addition. Averagely 30.1% decrease of *Geobacter* was observed on days 0–6, and the relative abundance remained under 0.85%. In contrast, the significant proliferation of SRB was observed with 3.51 times of increase in average comparing to the initial value. The dominating functional SRB genera were *Desulfobulbus* and *Desulfatiglans* (Fig. 6). Sulfate reducers including 18 classified genera counted for 3.55% of relative abundance in treatment with highest amended sulfate. This proportion was 2.75, 2.46 times iron-reducing and methanogenesis functional genera respectively. In addition, a divergence between sulfide-oxidizing bacteria and sulfur-oxidizing bacteria was observed. 69.28% and 67.30% decreases of sulfide-oxidizing bacteria were found on days 6 and 12 on average while 3.05 times increase of dominated sulfur-oxidizing genera *Thiobacillus* was observed on day 6. The relative abundance of *Thiobacillus* was up to 1.24% on day 6.

According to result from RT-QPCR, SRB numbers generally exhibited similar arched shape in all treatments (Fig. 7). Strong increases on days 0–6 were observed comparing to initial values. Although the SRB numbers decreased during the later period of incubation, the final values were still 566.49 (1.5S) – 3603.27% (3.0S) higher than the initial values. Elevated sulfate levels have great impacts on SRB distribution. The increase of SRB numbers was concurrent with sulfate addition. The peak values in surface sediments were 60.18 (1.5S), 79.35 (2.0S), 77.03 (2.5S), 170.55 (3.0S) folds comparing to day 0, respectively. In addition, the date reaching the peak value of 1.5 and 2.0S treatments was earlier than 2.5 and 3.0S, which indicated that increasing sulfate lengthened the thriving duration of SRB population.

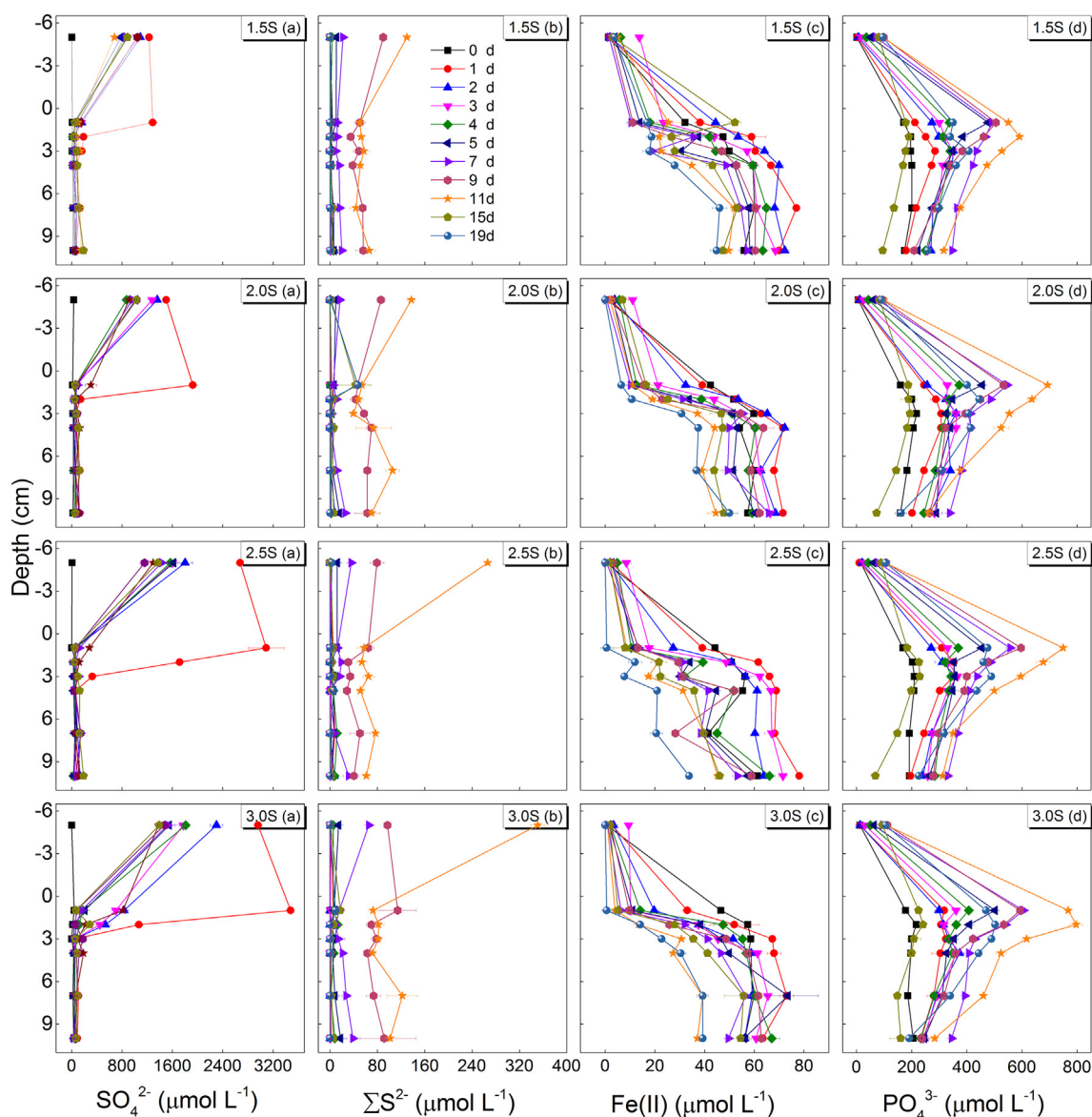


Fig. 4. Variations of  $\text{SO}_4^{2-}$  (a),  $\Sigma\text{S}^{2-}$  (b), Fe(II) (c) and  $\text{PO}_4^{3-}$  (d) in sediment pore-water.

#### 4. Discussion

There have been many studies on the intrinsic link among the sulfur, iron, and phosphorus cycling in aquatic ecosystems (Dang and Lovell, 2016; Ding et al., 2016; Friedrich and Finster, 2014; Hansel et al., 2015; Zhao et al., 2019). Recent reports have further focused on the effects of sulfate reduction in freshwater sediments, demonstrating that the sulfate reduction process might stimulate phosphorus release in sediments by influencing the iron cycling (Chen et al., 2016; Zhao et al., 2019). However, since these systems all involved algae decomposition, it is difficult to distinguish the source of inorganic elements (S, Fe, P) in the water column, whether it is from algae decomposition in the water column or phosphorus release in sediments. So it seems vital to provide direct evidence of sedimentary Fe-P mobilization caused by sulfate reduction. Here we demonstrate that sulfur cycling has a critical effect on iron cycling and could significantly stimulate phosphorus mobilization in sediments. For this, we provided direct evidence by carrying out a mesocosm experiment with the addition of acetate instead of algae for reducing condition and substrate supply, and carefully tracking the S, Fe and P dynamics in water column and sediments.

After acetate addition, immediate downtrends of DTC and DOC were observed (Fig. 1), which were attributed to the diffusion to sediments, enzymatic respiration and fermentation (Peng et al., 2011). Meanwhile, DO and ORP in the water column and sediments dramatically declined (Fig. 2), revealing the formation of anaerobic and reducing condition under the drive of the microbial degradation. To note, uptrends of ORP values with increasing depth were observed during the first ten days (Fig. 2b), which were inverse to the classic depth-dependence distribution reported previously (Han et al., 2015). This phenomenon indicated that more active microbial activities occurred in surface sediments rather than deeper sediments or water column. As the stronger resistance of ORP recovery was observed at higher amended sulfate, the microbial activities were related to sulfur species.

The biogeochemical processes of sulfur were significantly stimulated by acetate degradation and the resulting reducing condition in the system.  $\text{SO}_4^{2-}$  concentrations in overlying and pore water dropped rapidly after the acetate addition (Figs. 3a and 4a) while significant increases of  $\Sigma\text{S}^{2-}$  concentrations were observed in all treatments (Figs. 3b and 4b). These variations demonstrated that strong sulfate reduction occurred in the water column and sediments during acetate degradation, which

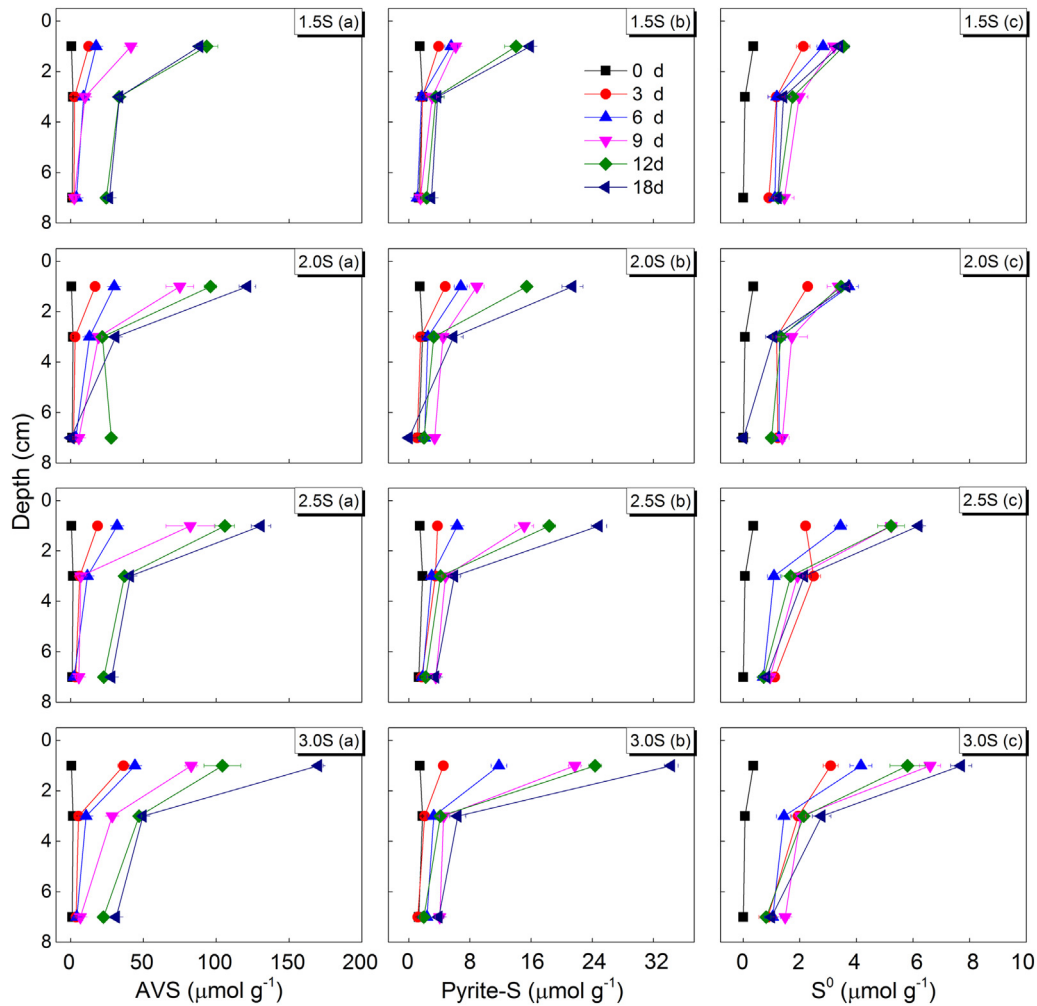


Fig. 5. Contents of AVS (a), pyrite-S (b),  $S^0$  (c) in surface sediments (0–1 cm).

was also confirmed by the dramatical increase of SRB abundance in the surface sediment (Fig. 7).

However, rapid drops of  $SO_2-4$  concentrations in both overlying and pore water were observed in all treatments during whole incubation while  $\Sigma S^{2-}$  increase in water column did not exist until day 6, and a stoichiometric magnitude mismatch between  $SO_2-4$  decrease and  $\Sigma S^{2-}$  increase was observed. The similar phenomenon has been reported in previous studies and the missing  $\Sigma S^{2-}$  was attributed to the precipitation of sedimentary sulfur (Baldwin and Mitchell, 2012; Friedrich and Finster, 2014). In this study, rapid accumulations of AVS and pyrite-S continuously proceeded during whole incubation, suggesting that the  $\Sigma S^{2-}$  produced by sulfate reduction might be the first to react with Fe(II) to form solid iron sulfides and be stored in sediments, rather than diffuse to overlying or pore water. Thus, the  $\Sigma S^{2-}$  formation in the liquid phase and the corresponding  $\Sigma S^{2-}$ -missing sulfur cycling seems “concealed” and “cryptic”. Similar sulfur cycling was observed in unexpected high rates of sulfate reduction within low-sulfate

sediments (Otero et al., 2006; Pester et al., 2012; Wijsman et al., 2001), and rates of sulfate reduction investigated on the basis of  $\Sigma S^{2-}$  variation in pore water will apparently lead to underestimation.

To further explore the sulfur cycling in sediments, microbial communities of sulfate reducers in the surface sediments were investigated. Results showed a significant proliferation of SRB in surface sediments with the dominating groups of *Desulfohalobus* and *Desulfatiglans* (Fig. 6), which were generally the main SRB species in freshwater ecosystems (Hansel et al., 2015). A total of 18 classified genera with sulfate-reducing function were detected, and their relative abundance was up to 3.55%, which was similar to the SRB populations in previously incubated sediments demonstrated with strong sulfate reduction (Chen et al., 2016). This value was much higher than the functional genera of iron-reducing and methanogen (Fig. 6), suggesting that SRB dominated the anaerobic respiration in surface sediments. Furthermore, the dramatical increase of SRB abundance in the surface sediment with the increasing sulfate level (Fig. 7) indicated that sulfate reducers in

Table 1  
Sedimentary iron and phosphorus on days 0 and 19.

Initial values ( $\mu\text{mol g}^{-1}$ , 0 d)	Values in the end of incubation ( $\mu\text{mol g}^{-1}$ )				
	1.5 s	2.0 s	2.5 s	3.0 s	
Fe-P	$9.46 \pm 0.27$	$8.71 \pm 0.17$	$7.84 \pm 0.29$	$6.31 \pm 0.21$	$6.15 \pm 0.33$
TP	$37.83 \pm 1.10$	$37.12 \pm 1.15$	$33.20 \pm 0.71$	$31.38 \pm 0.92$	$30.09 \pm 0.38$
Ferrihydrite-Fe	$80.26 \pm 9.72$	$70.47 \pm 5.42$	$72.58 \pm 10.28$	$62.41 \pm 2.06$	$59.72 \pm 6.06$
Total Fe(III)	$260.22 \pm 7.74$	$248.50 \pm 8.24$	$240.74 \pm 9.23$	$246.73 \pm 9.21$	$228.43 \pm 10.03$

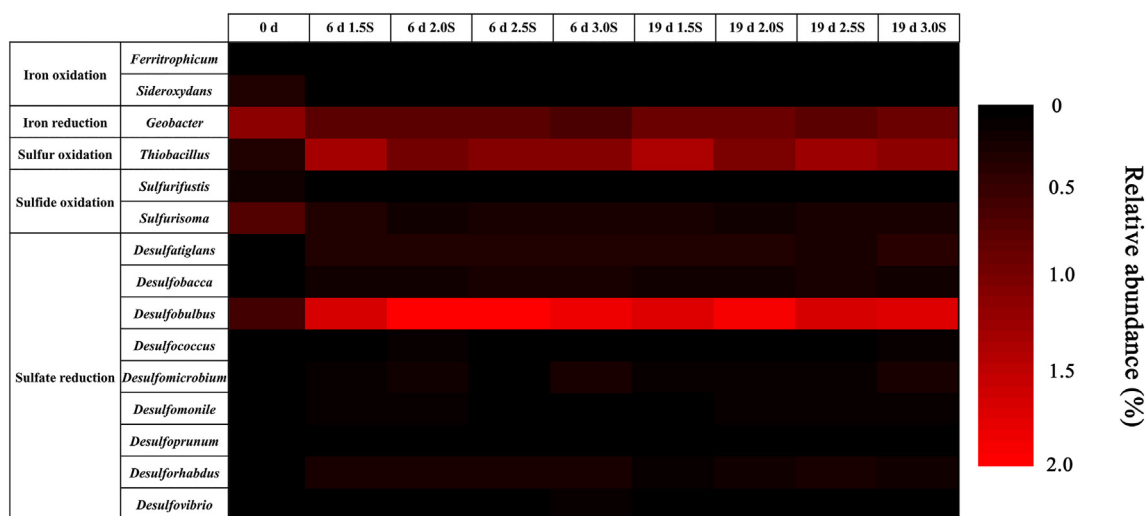


Fig. 6. Relative abundance of major iron and sulfur species (genera) in 0–1 cm sediments.

freshwater sediments with no history of exposure to high salt have sufficient capacities to survive under rapid increasing salinity (Rees et al., 2010). According to the matching distribution of SRB and sulfur species, it is obvious that acetate addition and formed reducing condition significantly stimulated SRB growth and the resulting sulfur reduction, allowing the  $\text{SO}_4^{2-}$  to precipitate in surface sediment as the solid sulfides continuously.

In the SRB-abundant sediments, the sulfate reduction was concededly the main pathway of sulfur cycling. However, sulfur cycling in this study was found neither single nor unidirectional.  $\text{S}^0$ , which was identified as a crucial intermediate reactant in sulfur cycling, continuously accumulated in surface sediments (Fig. 5c) (Friedrich and Finster, 2014). Correspondingly, the uptrend of sulfur-oxidizing genera *Thiobacillus* was found, suggesting that complex sulfur disproportionation occurred in surface sediments. Furthermore, the sulfide-oxidizing bacteria were also observed, which indicated the possible sulfide oxidation regardless of reducing conditions. Thus, according to the monitored sulfur species, sulfur cycling in this study is not merely the sulfate reduction to sulfide but contains a series of small reaction chains including sulfate reduction, sulfide oxidation, and sulfur disproportionation.

Stimulated sulfur cycling was also implicated in the variation of iron cycling. It could be proved that the iron reduction sustainably occurred in the system over the whole incubation by Fe(II) distributions in

overlying (Fig. 3c) and pore water (Fig. 4c), as well as the continuous accumulation of AVS and pyrite-S in surface sediments (Fig. 5a, b). According to the microbial community results shown in Fig. 6, *Geobacter* was the main reducer in surface sediments after preincubation, for its relative abundance was higher than that of sulfate-reducing species. Meanwhile, acidobacteria was also observed, which was demonstrated to have the function of iron reduction (Weber et al., 2006). Correspondingly, a sharp increase of Fe(II) concentration in the water column and sediment pore-water was observed at the initial stage, indicating that microbial iron reduction (MIR) driving by IRB was a crucial pathway of iron reduction process at the initial stage of organic matters decomposition (Kwon et al., 2016).

However, the continuous decline of Fe(II) in the pore and overlying water from day 3 revealed a subsequent suppression on Fe(II) release. Moreover, as ORP, an essential factor in the iron-reducing environment, declined with depth in this study (Fig. 2), expected enzymatic iron reduction should reveal a similar vertical distribution (Lentini et al., 2012). However, inverse patterns towards the expected vertical distribution of Fe(II) were observed, suggesting strong inhibition on Fe(II) release occurred in upper sediments. Correspondingly, the IRB population was gradually depressed, which reflected in the decreasing relative abundance of *Geobacter* to below 0.85% on day 6 (Fig. 6), even though the substrate supply and presence of ferrihydrite in surface sediments seemed sufficient. These results revealed a strong suppression of MIR. To note is that stronger inhibition on Fe(II) release was found at high sulfate levels. It is clear that sulfur cycling was involved. Similar cases of MIR inhibition have been reported and mostly attributed to the competition between SRB and IRB, as they had the same demand for reducing conditions and substrates (Hansel et al., 2015; Koretsky et al., 2003; Man et al., 2014). In this study, similar variations of increasing SRB and depressed IRB were observed (Figs. 6 and 7), which might be because of the higher affinity of SRB for most common substrates (Hansel et al., 2015; Man et al., 2014; Reyes et al., 2017). In addition, although it was reported that SRB could directly reduce iron oxides (Flynn et al., 2014; Friedrich and Finster, 2014), only 5% of iron oxides could be reduced by the SRB when  $\text{SO}_4^{2-}$  was not present (Li et al., 2006). Considering the low content of  $\text{SO}_4^{2-}$  in sediments, reduction of iron oxides by SRB was minor. Accordingly, SRB activities assumed the main responsibility for the depressed IRB and MIR.

Although MIR was suppressed, the iron reduction was still in progress with evidence of continuous dissolution of iron oxides. The rapid precipitation of iron sulfides was correspondingly observed (Fig. 5), suggesting that Fe(III) was continuously reduced and mostly buried as iron sulfides. Thus, sulfide-mediated chemical iron reduction (SCIR) obviously dominated the iron reduction instead of MIR. As reported in

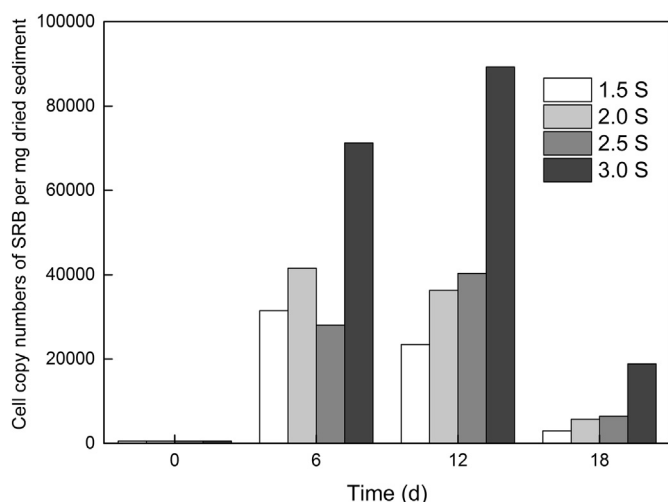


Fig. 7. Cell copy numbers of SRB in 0–1 cm sediments on days 0, 6, 12 and 18.

previous studies, the crucial difference between MIR and SCIR was the destination of reduced ferric ions, which ultimately dissolved into the water via the former pathway and precipitated with sulfide via latter pathway (Canfield, 1989; Lehtoranta et al., 2009). Without the dissolved Fe(II) generation, oxidation to Fe(III) is hard to realize. Thus, the iron cycling was blocked and turned into unidirectional SCIR. The lessening of the iron pool was observed in all treatments due to the continuous dissolution of iron oxides by SCIR, demonstrating the sulfide-induced uptake of iron oxides (Vali, 2006). Typically, ferrihydrite-Fe decreased by 25.59% after incubation in this study in treatment 3.0S (Table 1).

The phosphorus cycling would be inevitably affected by the variation of iron cycling, mainly reflecting in the mobility of phosphate in the sediment. As shown by the  $\text{PO}_4^{3-}$  distribution in the water column and sediment pore-water (Figs. 3d and 4d),  $\text{PO}_4^{3-}$  concentration gradually increased during the first 11 days after acetate addition followed by the stabilization, indicating the strong  $\text{PO}_4^{3-}$  release from sediments to the water column during the decomposition of organic matter. Obviously, the stimulated SCIR was expected to interfere in the pathway of phosphorus mobilization. Generally, ferric/ferrous oxides such as strengite ( $\text{FePO}_4 \cdot 2\text{H}_2\text{O}$ ) and vivianite ( $\text{Fe}_3(\text{PO}_4)_2 \cdot 8\text{H}_2\text{O}$ ) were commonly observed in sediments as a reservoir of phosphorus when sulfide is rare (Taylor and Konhauser, 2011). Because the microbial reductive dissolution of iron (hydr)oxides can lead to the  $\text{PO}_4^{3-}$  desorption and release, while the reoxidized Fe(III) will rebind the  $\text{PO}_4^{3-}$  and precipitate (Amirbahman et al., 2003). In this study, however, SCIR dominated the iron reduction instead of MIR, so that Fe(II) is continuously deposited as the solid iron sulfide species on the surface of sediment, resulting in the sustained release of  $\text{PO}_4^{3-}$ . Actually, we found that the eventual molar ratio of Fe(II) to  $\text{PO}_4^{3-}$  in sediment pore-water was 0.03 (3.0S group) - 0.09 (1.5S group), which was far below 2 that was the minimum value that released phosphorus could be totally re-bound by iron (Gunnars et al., 2002), confirming the diminished binding capacity to phosphorus due to the SCIR. In addition, it should be noted that more  $\text{PO}_4^{3-}$  release was observed at higher amended-sulfate treatment group (Figs. 3d and 4d), which means that the sulfate may directly affect the phosphorus mobilization in sediments by controlling the SCIR.

As is shown above, the switch of iron reduction from MIR to SCIR and consequent phosphorus mobility derived from the sulfur cycling could occur even under the current sulfate level in Lake Taihu. As algae blooms are common in eutrophic lakes, organic matter level during decomposition of algae residual is probably higher than the level in this study, which further provide substrates and reducing condition for SRB, similar cases might occur. Moreover, considering the preferential utilization of  $\text{S}^{2-}$  concealed sulfur cycling in this study, similar “cryptic” sulfur cycling could easily be neglected by merely measuring  $\text{SO}_4^{2-}$  and  $\text{S}^{2-}$ , especially in low-sulfate systems. Thus, the solid sulfides should also be considered when investigating the sulfur cycling of freshwater ecosystems. The results of this study will help broaden the understanding of sulfur cycling in the eutrophic freshwater ecosystem, and its mediated iron reduction and the closely related phosphorus release in the sediment.

## 5. Conclusion

The study showed the sulfur cycling and its impacts on iron and phosphorus with acetate addition under elevated sulfate levels ( $1.5\text{--}3.0\text{ mmol L}^{-1}$ ). Strong variations of  $\text{SO}_4^{2-}$  and  $\text{S}^{2-}$  suggested that current sulfate level in Lake Taihu was high enough to induce sulfur cycling with moderate acetate addition regardless of the ferrihydrite presence. Strong sulfate reduction, complex sulfur disproportionation and slight sulfide oxidation consisted of sulfur cycling in this study. Unexpectedly, depressed IRB was found in surface sediments and consequently, SCIR dominated iron reduction instead of MIR, which turned iron cycling including precipitation and dissolution of iron oxides into unidirectional SCIR. Continuous decreases of the iron pool due to SCIR were observed. Furthermore, variations of iron and sulfur species result

in stimulation on  $\text{PO}_4^{3-}$  mineralization and diminution of scavenging capacity to rebind  $\text{PO}_4^{3-}$ . Considering the sustained converting from iron oxides to iron sulfides, the transition is hard to reverse. Stimulation on SCIR and  $\text{PO}_4^{3-}$  release by elevated sulfate levels were observed. As seasonal algal blooms are common in eutrophic lakes, which would induce hypoxia and provide the carbon source for SRB, similar cases probably occur. Thus, the stimulated iron deposition and the resulting phosphorus release derived from the sulfur cycling should be paid more attention to in the treatment of eutrophic freshwater ecosystems.

## Acknowledgements

This work was supported by the National Natural Science Foundation of China (No. 41573061, 21407076), Research Projects of Water Environment Comprehensive Management in Taihu Lake of Jiangsu Province (No. TH2014402), the Natural Science Foundation of the Higher Education Institutions of Jiangsu Province, China (No. 18KJB610011) and the Major Science and Technology Program for Water Pollution Control and Treatment (No. 2017ZX07203-003).

## References

- Amirbahman, A., Pearce, A.R., Bouchard, R.J., Norton, S.A., Kahl, J.S., 2003. Relationship between hypolimnetic phosphorus and iron release from eleven lakes in Maine, USA. *Biogeochemistry* 65 (3), 369–385.
- Anderson, D.M., Burkholder, J.M., Cochlan, W.P., Glibert, P.M., Gobler, C.J., Heil, C.A., Kudela, R., Parsons, M.L., Rensel, J.E., Townsend, D.W., 2009. Harmful algal blooms and eutrophication: examining linkages from selected coastal regions of the United States. *Harmful Algae* 8 (1), 39–53.
- Baldwin, D.S., Mitchell, A., 2012. Impact of sulfate pollution on anaerobic biogeochemical cycles in a wetland sediment. *Water Res.* 46 (4), 965–974.
- Bo, T., 2000. Bacterial manganese and iron reduction in aquatic sediments. *Adv. Microb. Ecol.* 16 (1), 41–84.
- Canfield, D.E., 1989. Reactive iron in marine sediments. *Geochim. Cosmochim. Acta* 53 (3), 619–632.
- Chen, M., Li, X.H., He, Y.H., Song, N., Cai, H.Y., Wang, C., Li, Y.T., Chu, H.Y., Krumholz, L.R., Jiang, H.L., 2016. Increasing sulfate concentrations result in higher sulfide production and phosphorus mobilization in a shallow eutrophic freshwater lake. *Water Res.* 96, 94–104.
- Chen, M., Ding, S., Chen, X., Sun, Q., Fan, X., Lin, J., Ren, M., Yang, L., Zhang, C., 2018. Mechanisms driving phosphorus release during algal blooms based on hourly changes in iron and phosphorus concentrations in sediments. *Water Res.* 133, 153–164.
- Cline, J.D., 1969. Spectrophotometric determination of hydrogen sulfide in natural waters. *Limnol. Oceanogr.* 14 (3), 454–458.
- Conley, D.J., Paerl, H.W., Howarth, R.W., Boesch, D.F., Seitzinger, S.P., Havens, K.E., Lancelot, C., Likens, G.E., 2009. Controlling eutrophication: nitrogen and phosphorus. *Science* 323 (5917), 1014–1015.
- Correll, D.L., David, L., 1998. Role of phosphorus in the eutrophication of receiving waters: a review. *J. Environ. Qual.* 27 (2), 261–266.
- Dang, H., Lovell, C.R., 2016. Microbial surface colonization and biofilm development in marine environments. *Microbiol. Mol. Biol. Rev.* 80 (1), 91–138.
- Diaz, R.J., Rosenberg, R., 2008. Spreading dead zones and consequences for marine ecosystems. *Science* 321 (5891), 926–929.
- Ding, S., Wang, Y., Wang, D., Li, Y.Y., Gong, M., Zhang, C., 2016. In situ, high-resolution evidence for iron-coupled mobilization of phosphorus in sediments. *Sci. Rep.* 6 (1).
- Flores-Alsina, X., Solon, K., Mbamba, C.K., et al., 2016. Modelling phosphorus (P), sulfur (S) and iron (Fe) interactions for dynamic simulations of anaerobic digestion processes. *Water Res.* 95, 370–382.
- Flynn, T.M., O’Loughlin, E.J., Mishra, B., Dichristina, T.J., Kemner, K.M., 2014. Sulfur-mediated electron shuttling during bacterial iron reduction. *Science* 344 (6187), 1039–1042.
- Friedrich, M.W., Finster, K.W., 2014. How sulfur beats iron. *Science* 344 (6187), 974–975.
- Glombitza, C., Adhikari, R.R., Riedinger, N., et al., 2016. Microbial sulfate reduction potential in coal-bearing sediments down to ~2.5 km below the seafloor off Shimokita Peninsula, Japan. *Front. Microbiol.* 7, 15.
- Gunnars, A., Blomqvist, S., Johansson, P., Andersson, C., 2002. Formation of Fe(III) oxyhydroxide colloids in freshwater and brackish seawater, with incorporation of phosphate and calcium. *Geochim. Cosmochim. Acta* 66 (5), 745–758.
- Hall, K.C., Baldwin, D.S., Rees, G.N., Richardson, A.J., 2006. Distribution of inland wetlands with sulfidic sediments in the Murray-Darling Basin, Australia. *Sci. Total Environ.* 370 (1), 235–244.
- Han, C., Ding, S., Yao, L., Shen, Q., Zhu, C., Wang, Y., Xu, D., 2015. Dynamics of phosphorus-iron-sulfur at the sediment-water interface influenced by algae blooms decomposition. *J. Hazard. Mater.* 300, 329–337.
- Hansel, C.M., Lentini, C.J., Tang, Y., Johnston, D.T., Wankel, S.D., Jardine, P.M., 2015. Dominance of sulfur-fueled iron oxide reduction in low-sulfate freshwater sediments. *ISME J.* 9 (11), 2400–2412.
- Hoehler, T.M., Alperin, M.J., Albert, D.B., Martens, C.S., 1998. Thermodynamic control on hydrogen concentrations in anoxic sediments. *Geochim. Cosmochim. Acta* 62 (10), 1745–1756.

- Hsieh, Y.P., Shieh, Y.N., 1997. Analysis of reduced inorganic sulfur by diffusion methods: improved apparatus and evaluation for sulfur isotopic studies. *Chem. Geol.* 137 (3), 255–261.
- Hyacinthe, C., Cappellen, P.V., 2004. An authigenic iron phosphate phase in estuarine sediments: composition, formation and chemical reactivity. *Mar. Chem.* 91 (1), 227–251.
- Koretsky, C.M., Moore, C.M., Lowe, K.L., Meile, C., Dichristina, T.J., Cappellen, P.V., 2003. Seasonal oscillation of microbial iron and sulfate reduction in saltmarsh sediments (Sapelo Island, GA, USA). *Biogeochemistry* 64 (2), 179–203.
- Kwon, M.J., O'Loughlin, Edward J., Boyanov, M.I., et al., 2016. Impact of organic carbon electron donors on microbial community development under iron- and sulfate-reducing conditions. *PLoS One* 11 (1).
- Lehtoranta, J., Ekholm, P., Pitkänen, H., 2009. Coastal eutrophication thresholds: a matter of sediment microbial processes. *Ambio* 38 (6), 303–308.
- Lentini, C.J., Wankel, S.D., Hansel, C.M., 2012. Enriched iron(III)-reducing bacterial communities are shaped by carbon substrate and Iron oxide mineralogy. *Front. Microbiol.* 3 (3), 404.
- Li, Y.L., Vali, H., Yang, J., Phelps, T.J., Zhang, C.L., 2006. Reduction of iron oxides enhanced by a sulfate-reducing bacterium and biogenic H<sub>2</sub>S. *Geomicrobiol. J.* 23 (2), 103–117.
- Lohmayer, R., Kappler, A., Lösekann-Behrens, T., Planer-Friedrich, B., 2014. Sulfur species as redox partners and electron shuttles for ferrihydrite reduction by *Sulfurospirillum deleyianum*. *Appl. Environ. Microbiol.* 80 (10), 3141–3149.
- Lovley, D.R., Phillips, E.J., 1988. Novel mode of microbial energy metabolism: organic carbon oxidation coupled to dissimilatory reduction of iron or manganese. *Appl. Environ. Microbiol.* 54 (6), 1472–1480.
- Man, J.K., Boyanov, M.I., Antonopoulos, D.A., Brulc, J.M., Johnston, E.R., Skinner, K.A., Kemner, K.M., O'Loughlin, E.J., 2014. Effects of dissimilatory sulfate reduction on Fe III (hydr)oxide reduction and microbial community development. *Geochim. Cosmochim. Acta* 129 (129), 177–190.
- Moosmann, L., Gachter, R., Muller, B., Wuest, A., 2006. Is phosphorus retention in autochthonous lake sediments controlled by oxygen or phosphorus. *Limnol. Oceanogr.* 51 (1), 763–771.
- Mort, H.P., Slomp, C.P., Bo, G.G., Andersen, T.J., 2010. Phosphorus recycling and burial in Baltic Sea sediments with contrasting redox conditions. *Geochim. Cosmochim. Acta* 74 (4), 1350–1362.
- Murphy, J., Riley, J., Riley, J., 1962. A Modified Single Solution for Determination of Phosphate in Nature Waters.
- Nakagawa, M., Ueno, Y., Hattori, S., Umemura, M., Yagi, A., Takai, K., Koba, K., Sasaki, Y., Makabe, A., Yoshida, N., 2012. Seasonal change in microbial sulfur cycling in monomictic Lake Fukami-ike, Japan. *Limnol. Oceanogr.* 57 (4), 974–988.
- Olsson, S., Regnéll, J., Persson, A., Sandgren, P., 1997. Sediment-chemistry response to land-use change and pollutant loading in a hypertrophic lake, southern Sweden. *J. Paleolimnol.* 17 (3), 275–294.
- Otero, X.L., Ferreira, T.O., Vidal-Torrado, P., Macías, F., 2006. Spatial variation in pore water geochemistry in a mangrove system (Pai Matos island, Cananea-Brazil). *Appl. Geochem.* 21 (12), 2171–2186.
- Paerl, H.W., Paul, V.J., 2012. Climate change: links to global expansion of harmful cyanobacteria. *Water Res.* 46 (5), 1349–1363.
- Patrick, W.H., Henderson, R.E., 1981. Reduction and reoxidation cycles of manganese and iron in flooded soil and in water solution. *Soil Sci. Soc. Am. J.* 45 (5), 855–859.
- Peng, X., Guo, L., Tian, W., Wu, Q.L., 2011. Novel *Clostridium* populations involved in the anaerobic degradation of *Microcystis* blooms. *ISME J.* 5 (5), 792–800.
- Pester, M., Knorr, K.H., Friedrich, M.W., Wagner, M., Loy, A., 2012. Sulfate-reducing microorganisms in wetlands – fameless actors in carbon cycling and climate change. *Front. Microbiol.* 3 (72), 72.
- Qin, B., Xu, P., Wu, Q., Luo, L., Zhang, Y., 2007. Environmental issues of Lake Taihu, China. *Hydrobiologia* 581 (1), 3–14.
- Rees, G.N., Baldwin, D.S., Watson, G.O., Hall, K.C., 2010. Sulfide formation in freshwater sediments, by sulfate-reducing microorganisms with diverse tolerance to salt. *Sci. Total Environ.* 409 (1), 134–139.
- Reyes, C., Schneider, D., Thurmer, A., et al., 2017. Potentially active iron, sulfur, and sulfate reducing bacteria in Skagerrak and Bothnian Bay sediments. *Geomicrobiol. J.* 34 (10), 840–850.
- Rozañ, T.F., Taillefert, M., Trouwborst, R.E., Glazer, B.T., Ma, S., Herszage, J., Valdes, L.M., Price, K.S., Luther, G.W., 2002. Iron-sulfur-phosphorus cycling in the sediments of a shallow coastal bay: implications for sediment nutrient release and benthic macroalgal blooms. *Limnol. Oceanogr.* 47 (5), 1346–1354.
- Schobben, M., Stebbins, A., Ghaderi, A., et al., 2016. Eutrophication, microbial-sulfate reduction and mass extinctions. *Commun. Integr. Biol.* 9 (1).
- Straub, K.L., Schink, B., 2004. Ferrihydrite-dependent growth of *Sulfurospirillum deleyianum* through electron transfer via sulfur cycling. *Appl. Environ. Microbiol.* 70 (10), 5744–5749.
- Tabatabai, M.A., 1974. A rapid method for determination of sulfate in water samples. *Environ. Lett.* 7 (3), 237–243.
- Taylor, K.G., Konhauser, K.O., 2011. Iron in earth surface systems: a major player in chemical and biological processes. *Elements* 7 (2), 83–88.
- Thamdrup, B., Fossing, H., Jørgensen, B.B., 1994. Manganese, iron and sulfur cycling in a coastal marine sediment, Aarhus bay, Denmark. *Geochim. Cosmochim. Acta* 58 (23), 5115–5129.
- Vali, H., 2006. Reduction of iron oxides enhanced by a sulfate-reducing bacterium and biogenic HS. *Geomicrobiol. J.* 23 (2), 103–117.
- Weber, K.A., Achenbach, L.A., Coates, J.D., 2006. Microorganisms pumping iron: anaerobic microbial iron oxidation and reduction. *Nat. Rev. Microbiol.* 4 (10), 752–764.
- Wijsman, J.W.M., Middelburg, J.J., Herman, P.M.J., Böttcher, M.E., Heip, C.H.R., 2001. Sulfur and iron speciation in surface sediments along the northwestern margin of the Black Sea. *Mar. Chem.* 74 (4), 261–278.
- Zhao, Y., Zhang, Z., Wang, G., Li, X., Ma, J., Chen, S., Deng, H., Annalisa, O.-H., 2019. High sulfide production induced by algae decomposition and its potential stimulation to phosphorus mobility in sediment. *Sci. Total Environ.* 650 (Part 1), 163–172.